Day-Ahead Operation Scheduling for Microgrids Considering Conservation Voltage Reduction and Uncertainty-Based Demand Response Programs

Tahere Daemi*, Shahram Pourfarzin, Hamidreza Akbari

Department of Electrical Engineering, Yazd Branch, Islamic Azad University, Yazd, Iran, t.daemi@iauyazd.ac.ir

Abstract

The planning and operation of microgrids have become very important challenges in the electricity industry due to the expansion of distributed generation (DG) resources and the development of demand response programs (DRPs). Microgrids generally include renewable DG resources whose generation is random. This leads to uncertainty in system planning. This study discusses microgrid operation management considering DRPs and implementation of conservation voltage reduction (CVR) in the future operation horizon. For this purpose, a stochastic operation planning model for the next day is designed, which is associated with the implementation of DRPs, CVR, and the presence of DG resources to optimize the performance of a smart microgrid to increase reliability and reduce costs. In this study, DRPs are implemented using time-of-use (TOU) and incentive-based programs. Incentive-based programs are used to deal with uncertainty in the commitment of renewable resources, and TOU programs are used to deal with the fluctuation of generation of renewable resources by establishing a relationship between uncertainty and the fluctuation of generation of these resources. Besides, CVR is applied and voltage-dependent load modeling is performed considering innovation in addition to the format of DRPs to further reduce peak loads. The uncertainty of DG resources is modeled using the information-gap decision theory (IGDT) method. This optimization is carried out on a sample microgrid using genetic algorithm (GA). According to the results, the implementation of uncertainty-based DRPs leads to cost reduction and improvement of microgrid reliability.

Keywords: Demand Response, Uncertainty, CVR, IGDT
Article history: Received 2023/10/08; Revised 2024/03/01; Accepted 2024/03/14, Article Type: Research paper

1. Introduction

Microgrids (MGs) have emerged as a promising solution to address the challenges associated with modern power distribution systems. They offer enhanced reliability, resilience, and energy efficiency. Conservation Voltage Reduction (CVR) is a key technique within microgrid planning that optimizes voltage levels to reduce energy consumption without compromising the quality of power delivered to end-users. The increasing demand for electricity, coupled with environmental concerns, has necessitated the development of sustainable and efficient power distribution solutions. Microgrids, which are localized, controllable, and often renewable-energy integrated systems, have gained importance for their potential to revolutionize the way we distribute and consume electrical energy. Within the framework of microgrid planning, the incorporation of CVR has become a crucial strategy for achieving energy efficiency goals [1]. CVR is a vital methodology employed in the delivery systems to guarantee that the voltage outline of the network remains within an acceptable range, as decided by the regulations established by the utility. Voltage regulation (VR) can be executed in various ways based on the conditions and demand of the system, and one such method is conservative voltage decrease (CVR), which entails decreasing the voltage level of the system or increasing it within the allowable range. CVR has garnered significant attention due to its potential to augment economic benefits and lessen costs linked to the functioning of power systems. By

adjusting the voltage outline of the delivery system, CVR can optimize the system's demand and increase the overall profitability of the network. Integrating CVR into microgrids offers several benefits [2]:

- Energy Savings: CVR reduces energy consumption by maintaining voltage levels closer to the optimal range for end-users, resulting in significant energy savings.
- Improved Grid Reliability: Microgrids with CVR enhance grid reliability by reducing voltage fluctuations and mitigating voltage-related issues, such as overvoltage or undervoltage.
- Enhanced Renewable Energy Integration: CVR helps stabilize voltage levels, facilitating the integration of intermittent renewable energy sources, such as solar and wind, into microgrid systems.
- Environmental Impact: Reduced energy consumption translates to lower greenhouse gas emissions and contributes to environmental sustainability.

Figure (1) represents a graphical representation of a system involving DG sources and VRs. In this context, DG sources likely refer to small-scale, decentralized energy generators such as solar panels, wind turbines, or geothermal systems. VRs are control devices that play a crucial role in regulating the voltage levels in the system, ensuring that they remain within acceptable limits. The figure highlights two distinct types of signals, color-coded for clarity. Signals depicted in red are associated with the production resources, which are presumably the DG sources. These red signals are indicative of the incentives provided by the electricity distribution company to encourage and support the operation of DG sources. Such incentives may encompass feed-in tariffs, net metering programs, or other financial mechanisms designed to promote renewable energy generation and reduce dependence on traditional grid sources. In contrast, the green signals in the figure are applied to loads within the system. These loads are characterized as being capable of participating in DR programs and implementing CVR strategies. DR programs typically involve adjusting electricity consumption patterns in response to grid conditions or price signals. By participating in DR, consumers can reduce their energy consumption during peak periods or when grid reliability is at risk. The application of green signals to these loads suggests a coordinated approach to managing electricity demand by encouraging load reduction and voltage optimization through CVR techniques.

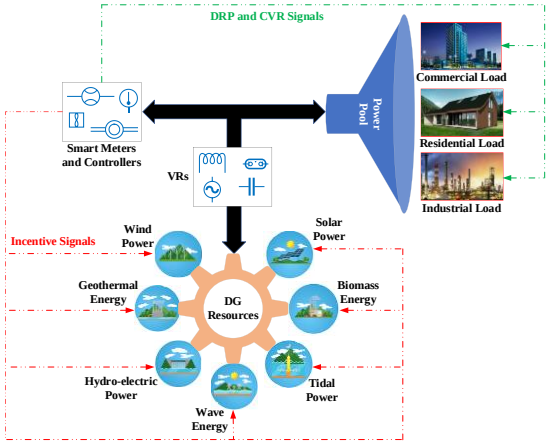

Fig. 1. A graphical representation of a MG involving DG sources and VRs implementing DRPs and CVR

CVR, has been extensively researched as a practical strategy for reducing peak loads, minimizing power losses, conserving energy, reducing operational expenses, and enhancing the dependability and security of power systems. In numerous studies, including a survey conducted in [3], the various applications of CVR and its potential to achieve economic operation and energy conservation have examined. In another study, the benefits and drawbacks of implementing CVR, its impact on cost reduction and energy conservation in power systems are discussed [4]. In [5], CVR was utilized to optimize the planning of a microgrid, determining the optimal placement and size of capacitors and distributed generations to enhance branch efficiency. Furthermore, [6] explored the energy-saving effects of implementing CVR and voltage optimization on the Ireland distribution system. The utilization of CVR to diminish energy usage and limit the maximum demand has been shown in [7]. In urgent situations where electrical energy availability is scarce to meet network demands, CVR can be employed to slightly reduce the demand, thereby enhancing the reliability and security of the power system. The effectiveness of CVR in enhancing power system stability, security, and reliability was assessed in [8]. In [9], the focus is on the growing energy requirements due to urbanization and technological progress, with a strong emphasis on the significance of incorporating renewable energy sources into conventional power grids. The paper conducts an assessment of optimization methods used for managing energy within microgrids, with a particular emphasis on the success of mixed integer programming, multi-agent-based approaches, and meta-heuristics. The depletion of natural resources and the intermittent nature of renewable energy sources have underscored the necessity for hybrid microgrids, merging AC and DC technologies to mitigate

deficiencies and enhance system reliability [10]. These hybrid microgrids align with the current trend of scattered and concentrated energy loads. This paper represents critical issues related to hybrid microgrids, including their integration, security, reliability, power generation optimization, load management in various scenarios, uncertainty management for renewable energy, feeder placement optimization, and cost-effective control strategies. The authors in [11] presents a coordinated strategy for optimizing voltage and VAR control in interconnected MGs and distributed energy resources (DERs), with a specific focus on conserving voltage levels but adaptable to other voltage-VAR optimization (VVO) challenges. It incorporates various voltage-power control modes of DERs at both the distribution network and MG levels. Validation on two test systems reveals that this approach, on average, enhances grid efficiency by 4% compared to scenarios based on economic operation [12-13]. Demand Response Program (DRP) is a valuable tool for distribution system operators as it can lower operational costs, enhance power system reliability, and increase profits from energy sales [14]. The Emergency Demand Response Program (EDRP) serves as a means to manage electricity prices during distribution system reliability issues. This research introduces a formulation that calculates the ideal demand levels within the EDRP, considering the perspective of the Regional Market Manager (RMM). The objective is to minimize EDRP costs and achieve load curve smoothing, employing a logarithmic model and a demand elasticity matrix [15]. Modifying the energy consumption pattern during a specific time frame can impact the voltage profile of the system. Previous studies [16-17] have explored the effects of DRP on voltage in distribution systems. In [18], emergency DRP was implemented to manage and regulate voltage in automated distribution networks in real-time. Given that the implementation of DRP in the distribution network can alter the voltage level, it is imperative to assess the impact of combining incentive-based DRP and ViR on the objective functions. The available literature highlights the importance of examining the effects of implementing DRP and ViR simultaneously in distribution systems [19]. DRP is an essential tool for improving the flexibility of energy systems to manage the unpredictable behavior of renewable generation and demand loads. In [20] the authors have proposed an integration DR strategy for the microgrid. Autonomous quotations based on electricity valuation were permitted to avoid disputes in the contribution clearing step. In addition, market clearing price with trading priority was specifically adopted to ensure incentive compatibility. The model presented in [21] investigates the impacts of CVR on electricity prices, the local market, and technical issues in distribution networks. An increase in electricity demand is one of the key challenges for developing sustainable societies. The authors in [22] aims to maintain voltage levels within standard ranges with optimal coordination of different resources at minimum operational costs and voltage deviation. The present investigation introduces a fresh VVM that is specially crafted for distribution networks to efficiently synchronize advanced grid technologies such as energy storage systems (ESSs), time-of-use demand response initiatives (TOU-DRP), and photovoltaic (PV) inverters with conventional tools like on-line tap changer transformers (OLTC) and switchable capacitor banks (SCBs). In [23], a stochastic design is suggested for ideal energy-heat programming and day-to-day storage of a MG. The bi-level stochastic programming design is created to combine energy-heat scheduling and storage while taking into consideration the presence of DR initiatives and ESSs for the purpose of optimizing social welfare. The main emphasis of the study lies in examining the impacts of several incentive-based DR initiatives.

This research makes significant contributions in several key aspects, which can be summarized as follows:

– Managing Wind Power Uncertainty: One notable contribution is addressing the inherent uncertainty in wind power generation forecasts. In practice, the actual wind power generation often deviates by a small amount (e.g., ±1 MW) from the predicted values. This research devises proportional DR contracts, employing diverse and efficient strategies, to cover this level of uncertainty, up to one MW. Furthermore, it recognizes the linear relationship between the average generation prediction and its standard deviation, thus enabling the formulation of DR contracts accommodating variations of up to two MW in cases where the average prediction is 18 MW. This dynamic approach differs from previous studies, where fixed uncertainty ranges was assumed, resulting in static DR contracts. By adapting contracts to the precise degree of uncertainty, this research mitigates both the risk of load shedding (which would incur load shedding penalties) and the potential escalation of system costs. Besided, this research innovatively models the uncertainty associated with renewable resources, particularly wind power, by establishing a relationship between the average and standard deviation of generation over time. The result is the allocation of DRPs that enhance system

reliability while optimizing microgrid operating costs.

- Incentive-Driven Load Participation: The study underscores that the primary driver motivating load participation in DRPs is the provision of suitable incentives. Importantly, these incentives are considered variable, thus emphasizing the importance of aligning incentives with load response.
- Renewable Resource Uncertainty Modeling: The main innovatio revolutionizes day-ahead operation scheduling for microgrids by integrating CVR and uncertainty-based demand response using IGDT. This method utilizes real-time optimization techniques to adaptively adjust schedules based on changing conditions, ensuring optimal energy usage and system reliability, results in maximizes energy efficiency, minimizes operational costs, and enhances the overall performance of microgrids.

The paper's structure is organized as follows: Section II Formulates the problem, elucidating the underlying objective functions and constraints. Section III Details the proposed approach for CVR and outlines the optimization algorithm employed. Section V Presents the simulation results and conducts an in-depth analysis. Finally, Section VI offers concluding remarks, summarizing the key findings and contributions of the research.

2. Model Characteristics and Objective Function

An optimization problem is developed in this study. So, it has an objective function and some constraints. The problem is relevant in the field of short-term studies of the power system. Thus, the time to solve it is very important. In the numerical results section, the solution time to solve a problem is proportional to the time horizon according to the proposed algorithms. The objective of this model is according to Equation (1) which expresses revenue and reliability as two objectives. So, the framework is multi-objective.

$$\text{maximizing}\left(\sum_{t=1}^{T}\sum_{i=1}^{I}\pi(t).P_{i,t} - Cost_{gen} - Cost_{res} - Cost_{rel} - C(P,\lambda)\right) \quad (1)$$

Where

$$Cost_{gen} = \sum_{t=1}^{T}\sum_{i=1}^{I}\left(C_{i,t}(P_{i,t},U_{i,t}) + SC_i.K_{i,t}\right) \quad (2)$$

$$Cost_{res} = \sum_{t=1}^{T}\sum_{i=1}^{I} q_{i,t}R_{i,t} \quad (3)$$

$$Cost_{rel} = EENS \times VOLL \quad (4)$$

The objective function of this study encompasses four primary components, establishing it as a multi-objective problem. The first component pertains to revenue, while the second focuses on generator charges. The revenue component is derived from the difference between income and expenses. Income, denoted by the first term, represents the revenue generated by supplying power to the upstream network. Total expenses encompass generation costs, spinning reserve costs, and reliability-related costs (Equation 4). The initial cost, comprising generation expenses and unit setup costs, is mathematically expressed in Equation (2). Spinning reserve costs are delineated in Equation (3) and moreover, the reliability cost is calculated as the product of load shedding and the value associated with lost load, often referred to as the outage penalty or load shedding penalty. This component is formally defined in Equation (4). In all equations, $\pi(t)$ represents the selling price of electricity to upstream network. The parameter $C(P,\lambda)$ represents the uncertainty reduction using IGDT method, which will be explained in Section 2.2. The next component within the objective function concerns the aspect of reliability, constituting the secondary objective of the problem. Reliability metrics in isolation may not adequately convey the network's reliability status. Consequently, the expected unsupplied energy index is converted into a cost metric by multiplying it with the value of the lost load. Additionally, the loss of load probability (LOLP) index is introduced as a distinct objective. In this context, the problem under consideration is bi-objective in nature. Equation (9) establishes an upper threshold for the load shedding probability index to ensure the attainment of a predetermined minimum level of reliability.

$$LOLP_t \le LOLP_t^{max} \quad (5)$$

Where $LOLP_t$ is the probability of hourly load shedding, and $LOLP_t^{max}$ is its permissible value. This constraint is intended to prevent the reliability index from exceeding a certain value. The constraint on generaion and consumption equilibrium is as follows:

$$\sum_{i=1}^{I} P_{i,t} = P_t^D \qquad \forall t = 1,\dots,T \quad (6)$$

In light of the inherent time constraints associated with each generating unit's ability to augment its power output, a fundamental limitation arises whereby it cannot instantaneously furnish the requisite reserve capacity. Consequently, it becomes imperative to incorporate and explicitly account for the ramp rate constraint, as delineated in (7).

$$R_{i,t} \le \min(U_{i,t}(RUR_i\tau), P_i^{max}U_{i,t} - P_{i,t}) \quad (7)$$

The energy storage system (ESS), represented by a battery, embodies a dispatchable unit endowed with the unique capability of both absorbing and supplying electrical power concurrently. This energy source adheres to a set of well-defined technical constraints, which are detailed as follows:

$$|P_t^E| \le P_{max}^E \quad (8)$$

$$C(t+1) = C(t) - d_T P_t^{Edc} \eta^E + \frac{d_T P_t^{Ec}}{\eta^E} \quad (9)$$

$$C(0) = C_S\,, C(T) = C_E \quad (10)$$

$$C_{min} \le C(t) \le C_{max} \quad (11)$$

Where $P_t^{Edc}$and P_t^{Ec} are discharge power and charge power, P_{max}^E is the maximum chargeable or discharge power of the battery, η^E is the charge or discharge efficiency, d_T is the duration in hours, $C(t)$ is the total vlaue of energy in the battery until hour t, C_S and C_E are the set values of battery energy at the beginning and end of the period, and C_{max} and C_{min} are the maximum and minimum battery capacity. Analogous to the ESS, the upstream grid possesses the dual capability of both power generation and consumption. The maximum capacity of this grid is contingent upon the capacity of its communication transformer interlinking it with the microgrid. Notably, the economic aspect of the upstream grid operation adheres to a principle where the cost incurred for either drawing power from this grid or supplying power to it corresponds to the prevailing wholesale market price.

A) Implementing DRP to the Model

As previously delineated, this study encompasses the evaluation of two distinct DRPs: incentive-based programs and Time-of-Use (TOU) programs. The fundamental objective is to ascertain that, following their participation in these programs, subscribers experience a discernible reduction in their electricity consumption costs as compared to a scenario in which they do not partake in said programs. This cost reduction is achieved while upholding the established comfort thresholds, thus effectively monitoring the propensity of loads to actively engage in these programs. The propensity of the DR system to optimize the electricity expenditure of consumers within each discrete time interval, where reductions or shading of the load schedule can be implemented, is mathematically expressed as follows [14-16].

$$Cost_{DR,i} = PD_i^t \times x_i^t \times EP_i^t \quad (12)$$

$$0.7 < x_i^t < 1 \quad (13)$$

Where EP^t is the price of electricity in each time interval t, PD^t is the electricity demand of shedabble loads at time t, and x^t is the decision variable for reducing the load and it is allowed to shed a maximum of 30% of the load. This variable has a value between 0.7 and 1. It is worth mentioning that with each amount of load shedding, an incentive equal to the price of electricity at that moment is given to the corresponding load. The second category of demand response mechanisms, which operate in response to price signals, encompasses three distinct modalities: TOU, Real-Time Pricing (RTP), and Critical Peak Pricing (CPP). These modalities collectively influence the cost dynamics associated with supplying electricity to meet responsive demand. Specifically, they reflect pricing models akin to the TOU program and real-time market pricing. The precise valuation of this cost is determined through the mathematical formulations provided in Equations (14) and (15). These equations encapsulate the essential computational underpinnings governing the cost dynamics associated with fulfilling responsive demand in alignment with the TOU program and actual market pricing.

$$Cost_{DR,total} = \left(1 - (\gamma_1 + \gamma_2 + \gamma_3)\right) K_1$$

$$K_1 = \sum_{i=1}^{N_{customers}} \sum_{t=1}^{T} EP_i^t\, d_0(t) + \sum_{t=1}^{T} \rho(t)\, d_e(t) \quad (14)$$

$$d_e(t) = (\gamma_1 + \gamma_2 + \gamma_3) * d_0(t)\, \mathrm{K}_2$$

$$K_2 = \left(1 + \sum_{k=1}^{T} E(t.k) * \frac{\rho(k) - EP^t}{EP^t}\right) \quad (15)$$

The allocation of shiftable loads across distinct demand response programs is a variable endeavor, denoting that a portion of these loads is attributed to the TOU program, another fraction to RTP program, and yet another segment to the CPP program. Collectively, the sum of these fractions equals 1, signifying complete allocation. For the TOU and CPP programs, Equation (14) characterizes their cost calculation framework, marking a commonality between these two programs. The sole distinction between these programs, as highlighted in Equation (15), is encapsulated within the design of the pricing function denoted as $\rho(k)$. Within the TOU program, a tiered tariff structure encompassing off-peak, mid-peak, and on-peak hours is applied. Conversely, the RTP program introduces an hourly dynamic in this tariff structure. In the equations presented, γ_1, γ_2 and γ_3 signify the percentage participation rates in the RTP, TOU, and CPP programs, respectively. Moreover, de(t) represents the consumption of price-sensitive subscribers at hour t following their program engagement, while $d_0(t)$ denotes the consumption of shiftable loads prior to program participation. $E(t.k)$ is the price elasticity coefficient between hour t and hour k, and ρ(t) is the electricity tariff at hour t, with ρ_0 representing the initial price at hour t. It is essential to underscore that both the hourly tariff schedule and the percentage of subscriber participation necessitate determination as part of the overarching optimization problem, facilitating the optimal design of the responsive demand program. Notably, the primary distinction between the TOU and RTP programs is rooted in the type of elasticity matrix, which will be elaborated upon in subsequent chapters, particularly in the section dedicated to simulation. In accordance with the Cobb-Douglas production function framework, the consumption behavior of subscribers is conceptualized as a

function reliant upon temperature and price parameters. This modeling approach is employed to elucidate the impact of peak pricing strategies on the electricity consumption patterns exhibited by subscribers, as expounded upon in [7], that formulated in (16) and (17). The Cobb-Douglas production function is a well-established mathematical model frequently employed in economics and related fields. Within this context, it serves as a powerful tool for explicating how variations in temperature and electricity price, both key determinants, influence the consumption patterns of subscribers. This approach allows for a more granular and comprehensive examination of the intricate interplay between these factors, contributing to a deeper understanding of consumer behavior within the context of peak pricing dynamics.

$$Q(t) = A\,P^{ep}(t)W^{ew}(t) \quad (16)$$

$$A = \gamma_3 * d_0(t) \quad (17)$$

$Q(t)$ represents the electricity consumption of loads enrolled in the CPP program after program execution, while A signifies the constant coefficient associated with the load's intrinsic value, expressed as a percentage of the initial shiftable load. Within this framework, P represents the prevailing electricity price, and W stands for the ambient temperature. The parameters "ep" and "ew" denote the degree of dependence of electricity consumption on price and temperature, respectively. It is important to underscore those variations in these parameters hold significant implications for consumption behavior. Specifically, as the electricity price escalates, there is an associated decrement in consumption, while conversely, as ambient temperature rises, consumption tends to increase. This reflects the expected response of consumers to price and temperature fluctuations. To facilitate further analysis, we employ a logarithmic transformation of Equation (18), representing each variable with its respective small symbol. This logarithmic transformation serves as a mathematical tool to simplify and elucidate the underlying relationships between these variables, thereby aiding in the modeling and comprehension of consumption dynamics.

$$q(t) = A + ep * p(t) + ew * w(t) + U(t) \quad (18)$$

The stochastic error represented by U(t) is added to the equation to make the model more realistic. The parameters a, ep and ew are estimated by the least squares' method in such a way that Equation (19) is minimized (or consumption reduction is maximized).

$$\phi(a.ep.ew) = \sum_{i=1}^{T} U(t)^2 \sum_{i=1}^{T} \Big(q(t) - \big(a + ep * p(t) + ew * w(t)\big)\Big)^2 \quad (19)$$

In pursuit of this objective, a methodological approach entails the derivation of a system of simultaneous equations. This is accomplished by taking the derivative of the aforementioned parameters with respect to the variables of interest and subsequently setting these derivatives equal to zero. The rationale behind this approach is to identify equilibrium points or optimal values for the parameters of interest. The parameters under consideration can be effectively determined by solving this system of simultaneous equations in conjunction with historical data and information pertaining to the study system. This process harnesses both the mathematical relationships encapsulated within the equations and the empirical insights garnered from past observations, thereby enabling the calibration of the model and the estimation of parameter values. It is through this integrated approach that a comprehensive understanding of the system's behavior and the optimization of parameter values can be achieved.

B) DRP Uncertainty Modeling Using IGDT Method

The Information Gap Decision Theory (IGDT), abbreviated as IDGT, is a method used to address uncertainty in decision-making. It focuses on making decisions under conditions of limited or imperfect information. The primary aim of IDGT is to render the objective function, which relies on parameters characterized by uncertainty, more robust or flexible when confronted with input uncertainties. The presence of uncertainty parameters within a decision-making context can introduce a degree of unpredictability. On one hand, this unpredictability can potentially drive-up procurement costs, creating unfavorable conditions. On the other hand, it can also present opportunities for cost savings. In the IGDT approach, this inherent contradiction is effectively addressed by employing two distinct mathematical constructs: robustness and opportunity functions, as documented in [25]. The IGDT decision-making problem can be delineated into three essential components. Each of these components plays a crucial role in formulating the IGDT approach, enabling the development of strategies that strike a balance between robustness against unfavorable conditions and the exploitation of opportunities to minimize purchasing costs.

System Model: This component encompasses the representation of the system under consideration, including its key variables, constraints, and operating dynamics. In the context of uncertain parameters represented by λ and the decision variables denoted as P, the system model denoted as $C(P, \lambda)$ elucidates the interplay between inputs and outputs within the framework of the system model.

This system model is the foundation upon which the IGDT approach is employed. It is essential to emphasize that, in the context of this paper, the system model specifically pertains to the operational cost function of a MG in the presence of a DRP. To delve further into this, the system model encapsulates the intricate relationship between the uncertain parameters (λ), the decision variables (P), and the overarching objectives of optimizing the MG's operational cost in the presence of the DRP. It serves as the basis for making informed decisions that account for uncertainties, thereby ensuring efficient MG operations while considering the effects of DRP participation [25].

$$C(P,\lambda) = \sum_{t=1}^{T} \lambda_t \, P_t^{Grid} + \sum_{t=1}^{T} \sum_{s=1}^{N_s} \rho_s \times \sum_{j=1}^{N_j} \sum_{h=1}^{N_h} S_{j,h}^{MT} \, P_{j,h,t,s}^{MT} \quad (20)$$

Where

$$P_t^{Grid} + \sum_{j=1}^{N_j} \sum_{h=1}^{N_h} P_{j,h,t,s}^{MT} + P_{t,s}^{wind} + P_{(t,s)}^{PV} + P_{t,s}^{battery} = PD^t$$

Operational Requirements: Here, the specific operational objectives and constraints of the system are expressed, which are essential for achieving desired outcomes. The operation requirements refer to the specific criteria or anticipations set for the system under examination, often expressed as functions such as cost or other relevant metrics. In the context of the IGDT approach, these requirements are assessed using two key constructs: the robustness function and the opportunity function. Notably, in this context, the focus is on evaluating the operational cost of a MG. To elaborate further, the robustness and opportunity functions, as applied to the MG's operational cost problem, can be mathematically defined as follows, drawing from [25]:

- The robustness function provides insights into the system's ability to withstand adverse conditions and variations, offering a measure of resilience against unfavorable outcomes.
- The opportunity function explores the system's capacity to capitalize on favorable conditions or opportunities, shedding light on its potential for cost savings and efficiency improvements.

These functions play a pivotal role in the IGDT methodology, aiding decision-makers in assessing how well the system aligns with its operational objectives and how it responds to uncertainties in terms of operational cost, thus enabling informed and strategic decision-making.

$$\hat{\gamma} = max\{\gamma |\, maximum\ of\ the\ worst\ case\}$$
$$\hat{\theta} = min\{\theta |\, minimum\ of\ the\ best\ case\} \quad (21)$$

The concept of robustness in the face of uncertainty is gauged through the robustness function, assessing how well the system can withstand uncertainty without incurring high operational costs. This function also delineates the upper limit of uncertainty within which the minimum system requirements are consistently met, making a higher $\hat{\gamma}$ value preferable. In essence, the robustness function embodies a risk-averse approach to procurement strategy. This risk-aversion model can be mathematically expressed as an optimization function, denoted as (22), allowing for the systematic evaluation of robustness. Essentially, it quantifies the system's ability to maintain performance standards even in uncertain conditions and provides valuable insights into decision-making under uncertainty.

$$\hat{\gamma}(C_R) = max\{\gamma | max(C(P,\lambda)) < C_R\}$$
$$\hat{\gamma}(C_R) = max\left\{\frac{C_R - \sum_{t=1}^{T} \tilde{\lambda}_t \, P_t^{Grid} - \sum_{t=1}^{T} \sum_{s=1}^{N_s} \rho_s \times \sum_{j=1}^{N_j} \sum_{h=1}^{N_h} S_{j,h}^{MT} \, P_{j,h,t,s}^{MT}}{\sum_{t=1}^{T} \tilde{\lambda}_t \, P_t^{Grid}}\right\} \quad (22)$$

Where, $S_{j,h}^{MT}$ is related operation cost of generation block h of the jth unit of micro-turbine, P_t^{Grid} denoes imported power from the upstream grid to MG at time t and ρ_s shows the probability of scenario s if happened. The $P_{j,h,t,s}^{MT}$ represents the ower related to block h of the jth unit of micro-turbine at time t in scenario s. A decision is considered robust when it remains effective across a wide range of uncertainty parameters, and this robustness is particularly pronounced when $\hat{\gamma}(C_R)$ takes on a substantial value. Conversely, the opportunity function highlights the advantageous aspect of uncertainty parameters, offering opportunities to capitalize on lower prices from the upstream grid. Within this context, $\hat{\theta}$ is defined as the minimum value of γ that allows for the possibility of achieving cost-effective decisions. It's worth noting that the opportunity function identifies the minimum γ value that permits the MG to achieve an operational cost as low as a specified value, denoted as C_o. Therefore, a smaller $\hat{\theta}$ value is desirable as it signifies the potential for cost savings. A reduced $\hat{\theta}(C_o)$ indicates a scenario where benefits can be derived from lower upstream grid prices. The mathematical representation of the opportunity function in the IGDT approach is expressed as equation (23), with C_o typically being smaller than C_R. In essence, these functions help decision-makers assess the robustness of their decisions under uncertainty (robustness function) and identify opportunities for cost savings (opportunity function) within the context of MG operations and procurement strategies.

$$\hat{\theta}(C_o) = min\{\theta | min(C(P,\lambda)) < C_o\}$$
$$\hat{\theta}(C_o) = min\left\{\frac{\sum_{t=1}^{T} \tilde{\lambda}_t \, P_t^{Grid} + \sum_{t=1}^{T} \sum_{s=1}^{N_s} \rho_s \times \sum_{j=1}^{N_j} \sum_{h=1}^{N_h} S_{j,h}^{MT} \, P_{j,h,t,s}^{MT} - C_o}{\sum_{t=1}^{T} \tilde{\lambda}_t \, P_t^{Grid}}\right\} \quad (23)$$

Uncertainty Model: This component captures the uncertainties inherent in the system, encapsulating the various sources of unpredictability that could impact the decision-making process. The uncertainty model serves to quantify the disparity between the information we possess (typically forecasted data) and the information we lack (actual data). This gap is expressed as a function of specific parameters. In the case of a grid-connected MG, one crucial uncertainty is the upstream grid price, which significantly influences the MG's optimal bidding strategies. To capture this uncertainty, the IGDT approach introduces a fractional error as a means to model the uncertainty associated with the upstream grid price. This fractional error reflects the degree of divergence between the predicted and actual grid prices, shedding light on the MG's ability to adapt to price fluctuations and make informed bidding decisions. In essence, the uncertainty model, particularly in the context of grid-connected MGs, accounts for the discrepancies between forecasted and actual data, with a specific focus on the influential variable of upstream grid prices. It allows for a more realistic representation of uncertainties in the decision-making process for energy procurement and bidding strategies.

$$U(\gamma, \widetilde{\lambda_t}) = \left\{ \lambda_t | \left(\frac{|\lambda_t - \widetilde{\lambda_t}|}{\lambda_t} \right) < \gamma \right\} \quad (24)$$

The extent of the difference between the predicted upstream grid price (represented as $\widetilde{\lambda_t}$) and the actual grid price (denoted as λ_t) is characterized by the uncertainty parameter (γ). This parameter effectively quantifies the magnitude of uncertainty associated with grid prices, allowing decision-makers to assess and account for the variability between their forecasts and the real-world pricing dynamics.

C) Power Management Using CVR

One innovative approach to curbing energy consumption and peak load without disrupting the consumption patterns of subscribers is CVR This method achieves load reduction by carefully managing the voltage levels at consumption points, ensuring that system security remains intact. This is particularly significant since a substantial portion of the load directly correlates with voltage levels. Different types of loads respond differently to voltage variations. For example, cooling loads decrease their power consumption when voltage is lowered. However, they may take longer to reach the desired temperature since they operate with reduced power, leading to no net reduction in energy consumption. Conversely, another group of loads typically experiences both reduced energy consumption and power demand when voltage is lowered. Some loads, which maintain a constant power draw, show minimal responsiveness to voltage changes. Consequently, the effectiveness of CVR in a given grid depends on the load models and their characteristics. Research indicates that this method can yield energy consumption reductions ranging from 0.5% to 4%. To investigate the impact of CVR on optimizing microgrid usage, it is essential to consider grid load distribution equations alongside objective functions and constraints. The modeling of this problem encompasses various elements, including a radial grid structure model, voltage-dependent loads, on-load tap-changer (OLTC) transformers, and shunt capacitors. In a radial structure, the number of branches equals the number of nodes minus one. The initial bus, designated as bus number 0, serves as the connection point between the distribution grid and the transmission system, maintaining a constant voltage range. Consequently, load distribution equations for each branch can be formulated and analyzed in the context of optimizing microgrid operations as shown in (25) to (28).

$$P_{ij} - \sum_{k \in N_j} P_{jk} = \frac{r_{ij}\left(P_{ij}^2 + Q_{ij}^2\right)}{V_i^2} - p_j \quad (25)$$

$$Q_{ij} - \sum_{k \in N_j} Q_{jk} = \frac{x_{ij}\left(P_{ij}^2 + Q_{ij}^2\right)}{V_i^2} - q_j \quad (26)$$

$$V_i^2 - V_j^2 = 2\left(r_{ij}P_{ij} + x_{ij}Q_{ij}\right) - \frac{(r_{ij}^2 + x_{ij}^2)(P_{ij}^2 + Q_{ij}^2)}{V_i^2} \quad (27)$$

$$p_j = p_j^g - p_j^d \, , q_j = q_j^g - q_j^d + q_j^c \quad (28)$$

In this context, where i denotes the bus number, and p_j, q_j, and v_j represent the active power injection, reactive power injection, and voltage at that particular bus, respectively. Every line is characterized by a subscript ij, where r_{ij}, x_{ij}, P_{ij}, and Q_{ij} denote the resistance, reactance, active power flow, and reactive power flow for the line connecting buses i and j respectively. The superscript d signifies the load, and the load characteristics are modeled using the ZIP model. Consequently, the relationship between load values and voltage can be expressed through the following equations. To elaborate, this framework is essentially a representation of the electrical parameters and characteristics within a power distribution network. Each bus (node) in the network is assigned a number (i), and key electrical quantities like active power (p_j), reactive power (q_j), and voltage (v_j) are associated with these buses. Additionally, the transmission lines connecting these buses are denoted by 'ij,' and their properties, such as resistance r_{ij}, reactance (x_{ij}), active power flow (P_{ij}), and reactive power flow (Q_{ij}), are detailed. The d subscript signifies the load component, which is modeled using the ZIP model. The ZIP model provides a means to describe how

the load, which includes different types of appliances and devices, responds to changes in voltage. These models are crucial for understanding how the distribution of electrical power within the network affects the behavior of loads and helps in optimizing the operation of the system as formulated in (29) and (30).

$$p_j^d(V_j) = P_{0,j}^d \left[P_{Z,j} \left(\frac{V_j}{V_{0,j}} \right)^2 + P_{I,j} \left(\frac{V_j}{V_{0,j}} \right) + P_{P,j} \right] \quad (29)$$

$$q_j^d(V_j) = Q_{0,j}^d \left[Q_{Z,j} \left(\frac{V_j}{V_{0,j}} \right)^2 + Q_{I,j} \left(\frac{V_j}{V_{0,j}} \right) + Q_{P,j} \right] \quad (30)$$

Where the subscript 0 specifically represents the load value at nominal voltage, serving as a reference point for understanding load variations under different voltage conditions. The subscripts Z, I and P correspond to distinct load models:

- The subscript Z denotes the constant impedance model, where load behavior is influenced by variations in voltage, akin to how impedance responds to changes in electrical potential.
- The subscript I designates the constant current model, indicating that the load maintains a constant current irrespective of voltage fluctuations.
- The subscript P signifies the constant power model, in which the load maintains a consistent power draw regardless of voltage variations.

These different load models are essential for accurately representing how various types of loads in an electrical network respond to changes in voltage levels. Understanding these load characteristics is crucial for power system analysis and optimization. The transformer model, incorporating On-Load Tap Changer (OLTC), is represented as a component located between buses i and j. The concise power flow equations can be mathematically formulated as follows:

$$P_{ij} - \sum_{k \in N_j} P_{jk} = \frac{r_{ij}\left(P_{ij}^2 + Q_{ij}^2\right)}{V_i^2 / a_{ij}^2} - p_j \quad (31)$$

$$Q_{ij} - \sum_{k \in N_j} Q_{jk} = \frac{r_{ij}\left(P_{ij}^2 + Q_{ij}^2\right)}{V_i^2 / a_{ij}^2} - q_j \quad (32)$$

$$\frac{V_i^2}{a_{ij}^2} - V_j^2 = 2\left(r_{ij}P_{ij} + x_{ij}Q_{ij}\right) - \frac{\left(r_{ij}^2 + x_{ij}^2\right)\left(P_{ij}^2 + Q_{ij}^2\right)}{V_i^2 / a_{ij}^2} \quad (33)$$

$$\underline{a}_{ij} \le a_{ij} \le \overline{a}_{ij} \quad (34)$$

Where a_{ij} is the ratio of tap trans whose value is limited to a minimum and maximum range. Additionally, the inclusion of a shunt capacitor is represented as a parallel component with a susceptance connected to the respective bus. The magnitude of the injected reactive power from the shunt capacitor is contingent upon the voltage level. The susceptance value can be adjusted within the range from zero to its maximum allowable value. To expand further, a shunt capacitor is a device added to an electrical bus that can provide or absorb reactive power depending on the voltage conditions. Its reactive power output varies as a function of the bus voltage, and it can be controlled to enhance voltage stability and overall system performance. The parameter that characterizes this behavior is the susceptance, which can be adjusted to influence the magnitude of reactive power exchange. This flexibility allows for voltage regulation and improved system efficiency.

$$q_i^c(V_i) = B_i^c V_i^2 \quad (35)$$

$$0 \le B_i^c \le \overline{B_i^c} \quad (36)$$

In accordance with IEEE Std. 1547-2018, DG resources are categorized into two groups based on their reactive power capacity and their capability to control voltage. The first group comprises resources with limited voltage regulation capability that is within an acceptable range. This classification is typically applicable to systems with low penetration levels of DG resources. The second group encompasses resources with a higher capacity to regulate voltage, and this categorization is more relevant for systems with greater DG penetration. For the purposes of this study, we focus on resources with robust voltage control capabilities. These resources possess active and reactive power constraints determined by their capability curves, which can be expressed mathematically through equations (37) to (39). To provide a more comprehensive understanding, this categorization is essential in managing DG resources within the power system. Resources with advanced voltage control capabilities play a significant role in maintaining grid stability and ensuring voltage remains within acceptable limits. Their operational limits are described by mathematical expressions that help in optimizing their utilization within the power network.

$$a1_i^r s_i^r \le p_i^g \le a2_i^r s_i^r \quad (37)$$

$$b1_i^r p_i^g \le q_i^g \le b2_i^r p_i^g \quad (38)$$

$$c1_i^r s_i^r \le q_i^g \le c2_i^r s_i^r \quad (39)$$

In order to enhance the widespread implementation of CVR while upholding system reliability, the primary objective is to ensure that the voltage profile at any node remains within the lower acceptable limit. Maintaining the voltage within this constrained range takes precedence. To provide a deeper insight, the top priority in deploying CVR effectively while adhering to load shifting constraints is to ensure that the voltage levels at various nodes in the system are controlled within a specified lower bound. This voltage control is critical for system reliability. The voltage drop along

different sections of the distribution feeder can be comprehensively understood by analyzing the principles of power flow within the network. This knowledge is instrumental in optimizing CVR strategies while ensuring reliable operation. According to Figure (2), the voltage drop that occurs along any segment of the distribution feeder can be elucidated by considering the power flow characteristics, as follows [26]:

$$V_{j,t} = V_{i,t} + V_{tap} TAP_{ij} \quad (40)$$

$$TAP_{min} < TAP_{ij} < TAP_{max} \quad (41)$$

$$|V_{j,t} - V_{up}| < V_{threshold} \quad (42)$$

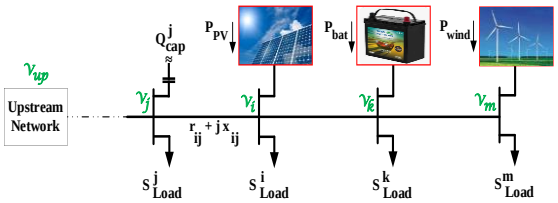

Fig. 2. Illustration of a radial electrical distribution test system

A step voltage regulator (SVR) situated at various points along the feeder is responsible for regulating the voltage at the immediate downstream node. This regulation is achieved by adjusting the tap settings as described in equations (40) and (42). When DR is employed for load reduction, customers may need to make compromises in their comfort to gain financial incentives. However, CVR operates differently; it's a utility-driven load reduction approach that involves lowering the operating voltage. This reduction, in turn, lowers consumption due to the load's sensitivity to voltage (known as Load to Voltage or LTV sensitivity). With CVR, there's no need for customer-side load reduction (or DR implementation). The decrease in consumption directly reduces customers' electricity bills, providing them with financial benefits without requiring them to compromise their comfort. DR can be effectively used for load shifting (LS) purposes. Utilities often offer various pricing schemes to customers, and a single scheme may not suit all customers because their usage patterns and load characteristics differ, depending on whether they are industrial, commercial, or residential customers. Additionally, different customers can have their loads shifted or scheduled at different times of the day based on predefined shifting criteria. Utilities can individually tailor optimal pricing schemes to provide customers with added economic benefits. Typically, these pricing schemes involve higher rates during peak periods, encouraging customers to shift their loads from peak to off-peak hours. Furthermore, rebate programs for peak-time usage can be implemented. By shifting loads, a more consistent voltage profile can be achieved, which enhances system reliability. This flattened voltage profile, achieved through Load Shifting-based Demand Response (LS-DR), facilitates CVR in maintaining an even lower operating voltage set point at the substation or feeder-head while ensuring a reasonable voltage profile along the feeder.

3. Simulation Results

Non-deterministic parameter scenarios, encompassing variables such as wind, load, and solar conditions, as well as pertinent data pertaining to generation resources, have been meticulously sourced and referenced as per [8]. The comprehensive grid topology information shall be furnished in the final phase of our numerical investigations, wherein the outcomes of CVR will undergo thorough analysis. It is imperative to underscore that this study centers on the numerical examination of a microgrid. To elucidate the operational framework, it is essential to delineate the essential parameters governing load and energy pricing within the upstream grid, as stipulated in [2]. Subscribers within the microgrid exhibit a consistent power consumption rate, quantified at 15 cents per kWh. The significance of the upstream grid rate is accentuated by the fact that power transactions between the microgrid and the broader grid adhere to this established rate. Elasticity matrices that underpin Time-of-Use (TOU) and Real-Time Pricing (RTP) programs have been sourced from [24], lending empirical rigor to our study's methodology. For visual clarity and reference, Figure (3) provides a graphical representation of the pricing structures associated with the aforementioned programs. Expanding upon the research, it is incumbent upon us to extend our examination to encompass the implications of these pricing structures on the microgrid's performance.

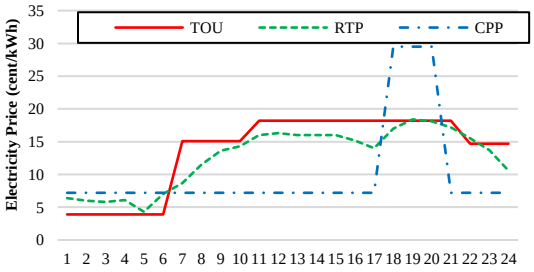

Fig. 3. Electricity price for TOU, RTP and CPP programs

Furthermore, a comprehensive analysis of the non-deterministic scenarios, including wind, load, and solar variations, is indispensable to elucidate the impact of CVR implementation within the microgrid. These multifaceted investigations shall contribute to a deeper understanding of the interplay between pricing mechanisms, renewable energy integration, and power exchange dynamics, thus

advancing the discourse on sustainable and efficient microgrid operation within the broader energy landscape.

A) Scenario 1: Without Effect of DRPs

The simulations in this study are carried out within the framework of several case studies to comprehensively explore the problem space. The presentation of simulation outcomes is systematically organized to facilitate a nuanced understanding of the optimization process. In Section 3.1.1, the simulation results are initially presented as single-objective outcomes, without considering the load shedding penalty. This approach provides insights into the system's performance when optimization is solely directed towards a primary objective, while the implications of load shedding are neglected. Subsequently, in Section 3.1.2, the analysis is extended by introducing the consideration of the load shedding penalty within the single-objective context. This enables a deeper examination of the trade-offs between the primary optimization objective and the load shedding penalty, shedding light on the implications of load shedding within the system. In the final stage of the analysis, the investigation is advanced to a multi-objective framework, as articulated in subsequent sections. Within this multi-objective paradigm, the load shedding penalty is systematically incorporated as a critical secondary objective. This holistic approach provides a comprehensive perspective on the interplay between multiple optimization objectives and the load shedding penalty, ultimately enhancing the understanding of the system's performance under diverse scenarios. By adopting this structured approach, the aim is to elucidate the complex dynamics governing the optimization process and the consequences of load shedding in various operational contexts. These insights contribute to a more profound comprehension of the system's behavior and inform decision-making processes for system optimization and resilience enhancement.

Case 1: No Load Shedding Penalty

In this section, critical information pertaining to the hourly load supply cost, generation rate, and reservation value for the GA optimization algorithms is provided. It is noteworthy that in this specific operational mode, a total cost of 15,778.67 cents is incurred. Furthermore, the hourly LOLP metric, a pivotal performance indicator, is graphically depicted in Figure (4) for comprehensive visualization and analysis. To extend our analysis, a detailed examination of the interplay between load supply costs, generation rates, and reservation values in the context of GA algorithms must be undertaken. A thorough understanding of these factors is deemed essential for the optimization of operational strategies and the promotion of cost-effectiveness within power distribution systems. Moreover, the graphical representation of LOLP in Figure (4) necessitates a more in-depth analysis to assess the system's reliability and resilience under varying load conditions. This holistic approach is considered vital for making informed decisions and enhancing the overall efficiency and stability of the power grid. This metric provides valuable insights into the efficiency and performance of the GA algorithm in mitigating energy losses. In the specific context of this analysis, it is established that the calculated expected value of lost energy over the course of 24 hours amounts to 0.187 kWh.

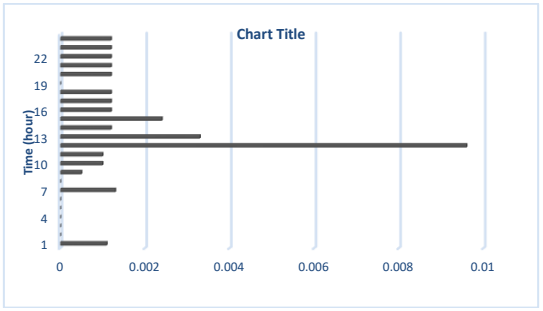

Fig. 4. Hourly LOLP with no load shedding penalty for case1

Case 2: Applying Load Shedding Penalty

Within the operational mode under scrutiny, the aggregate cost associated with delivering the requisite load is quantified at 16,703.97 cents. This financial metric represents a pivotal determinant in assessing the economic viability of the system's load supply strategy. Figure (5), prominently displayed, portrays the LOLP value, serving as a key performance indicator that sheds light on the system's reliability and robustness. In tandem with the aforementioned financial and reliability aspects, it is imperative to underscore that the expected value of lost energy is meticulously computed and registers at 0.357 kWh. This metric elucidates the energy efficiency aspects of the operational mode. Furthermore, it is imperative to emphasize the inherent conflict between two paramount objectives: the load interruption penalty and the reservation cost. These objectives present a challenging dichotomy that necessitates nuanced optimization strategies to strike an equilibrium between minimizing load interruptions and containing the reservation costs. In the quest for a comprehensive understanding of this complex dynamic, future inquiries may delve into the development of sophisticated optimization algorithms tailored to navigate this intricate trade-off, ultimately enhancing the operational efficiency and economic sustainability of the power system.

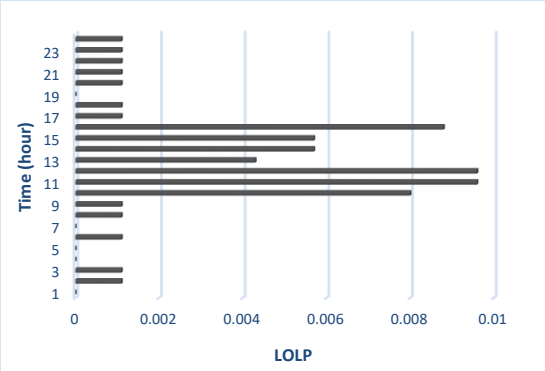

Fig. 5. Hourly LOLP with applying load shedding penalty for case 2

Case 3; Applying Multi Objective Load Shedding Penalty

In the context of this operational mode, the total cost incurred for the supply of load stands at 16,902.19 cents. This financial metric plays a pivotal role in assessing the economic aspects of load supply within this specific mode. Figure (6), which is prominently displayed, showcases the LOLP value, serving as a critical performance indicator that provides insights into the system's reliability and resilience. Besides, Figure (7) represents the hourly cost applying multi-objective load shedding penalty. In conjunction with the financial and reliability parameters, it is essential to underline that the expected value of lost energy is meticulously computed, resulting in a quantification of 0.263 kWh, along with an associated cost of 16902 cents. This metric offers a nuanced understanding of energy efficiency aspects within this operational context. To facilitate a comprehensive comparative analysis of the solutions derived from three distinct solution methodologies, we have tabulated the results in Table (1). This tabular presentation enables a detailed examination of the outcomes obtained through these methodologies. Upon careful scrutiny of Table (1), it becomes apparent that the cost exhibits an ascending trend. This trend is attributed to the absence of a load shedding penalty in the first case study and the allocation of reservation primarily to comply with the LOLP constraint. In contrast, the cost in the second case study, which incorporates a load shedding penalty in the objective function, exceeds that of the first study. This trend underscores the cost implications associated with incorporating load shedding penalties. Furthermore, it is noteworthy that the reliability value of cost increase in the second study registers an improvement when compared to the first study, further accentuating the role of the load shedding penalty in enhancing system reliability. Finally, the cost in the third study surpasses that of the second study, which is a single-objective optimization approach primarily focused on cost minimization. The third study, however, takes into account both reliability and cost objectives. This observation underscores the complex interplay between these objectives and the resulting trade-offs in optimizing load supply strategies. In future investigations, it is imperative to delve deeper into the underlying optimization methodologies and explore strategies that strike an optimal balance between cost minimization and reliability enhancement within the given operational context. In the realm of practical outcomes pertaining to DR and CVR, it is noteworthy to mention that the Mixed Integer Linear Programming (MILP) algorithm has yielded comparatively less robust results. It is essential to clarify that the focus here is not on the technical aspects of the algorithm itself, but rather on the tangible outcomes and implications of the DR and CVR strategies as applied in practice.

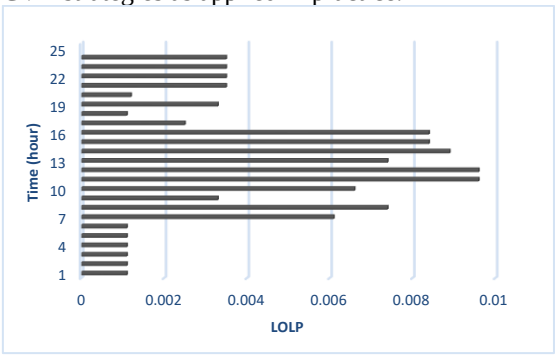

Fig. 6. Hourly LOLP with applying multi-objective load shedding penalty

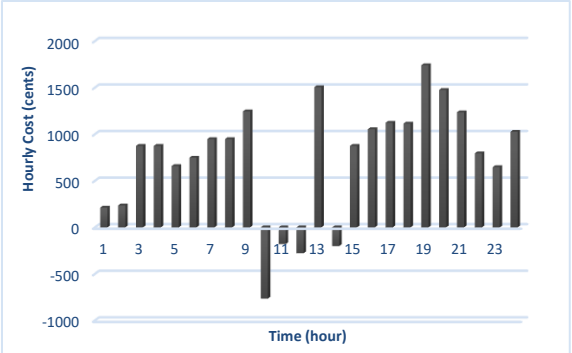

Fig. 7. Hourly cost applying multi-objective load shedding penalty

Table.1.
The comparison of solutions

Algorithm	*Without penalty or single objective (cents/kWh)*		*With penalty-single objective (cents/kWh)*		*Multi objective (cents/kWh)*	
	Cost	EENS	Cost	EENS	Cost	EENS
GA	15778	0.607	16702	0.478	16902	0.263
MILP	15998	0.685	17035	0.523	17475	0.362

B) Scenario 2: Considering the Effect of DRPs

In this scenario, the impact of DR implementation is considered for all case studies. The participation rate of subscribers in the CPP program, which is influenced by ambient temperature, is depicted in Figure (8). The modeling of CPP incorporates parameter values of *ep* (-0.83) and *ew* (1.2085). Figures (9) and (10) provide valuable insights into the TOU programs, where two distinct scenarios involving load curve modifications, namely, 5% and 10% variations, are applied. Additionally, the updated load profiles in response to shedding actions across various program components are presented in these figures. It should be noted that the critical peak values for ew and ep are maintained at 1.2085 and -0.83, respectively, within the pricing program's context. Furthermore, this comprehensive study is conducted under the purview of two distinct scenarios: one entailing a 5% participation rate in the TOU programs, and the other involving a 10% participation rate. This division is implemented to facilitate a more granular examination of the effects of varying participation levels within the TOU programs.

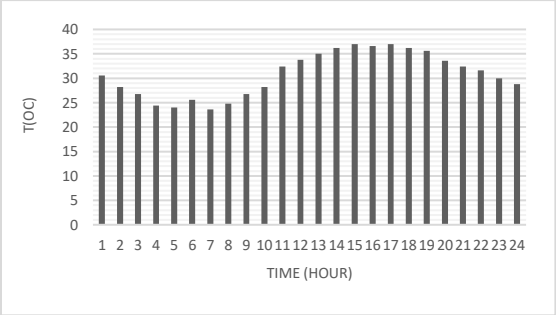

Fig. 8. The ambient temperature during 24 hours

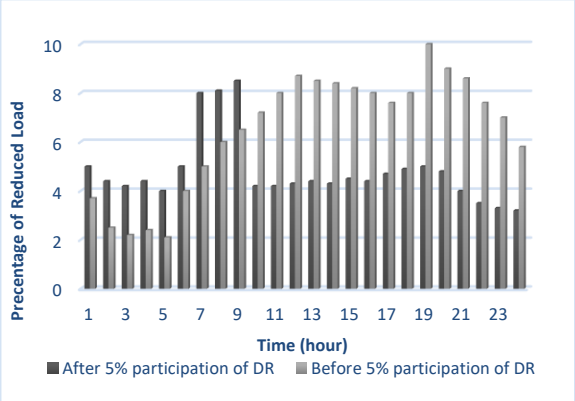

(a)

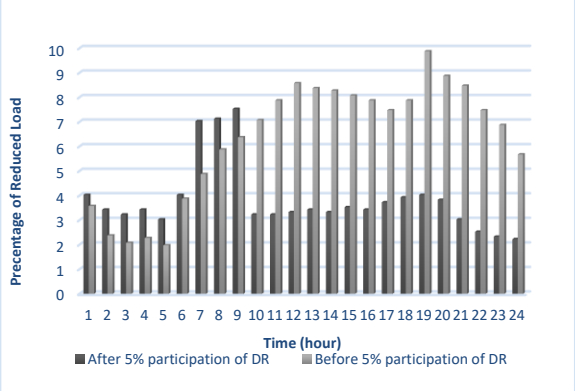

(b)

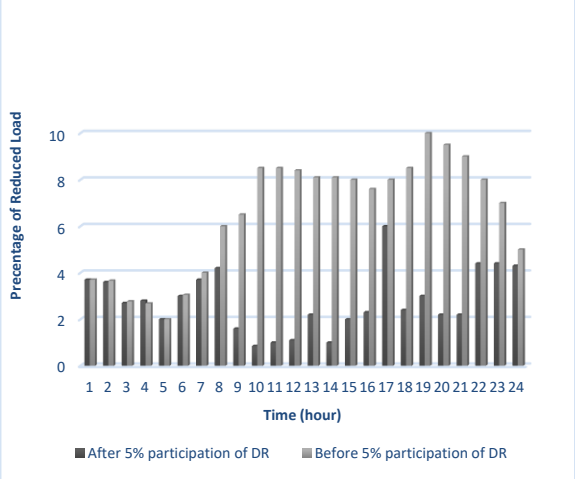

(c)

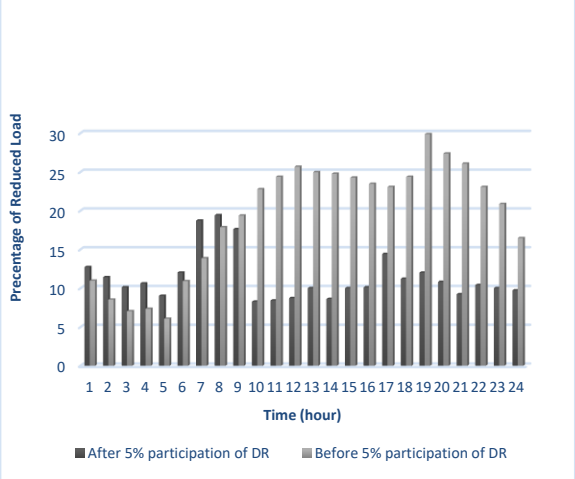

(d)

Fig. 9. Updated load for 5% participation of DR; a) TOU, b) RTP, c) CCP and d) total load

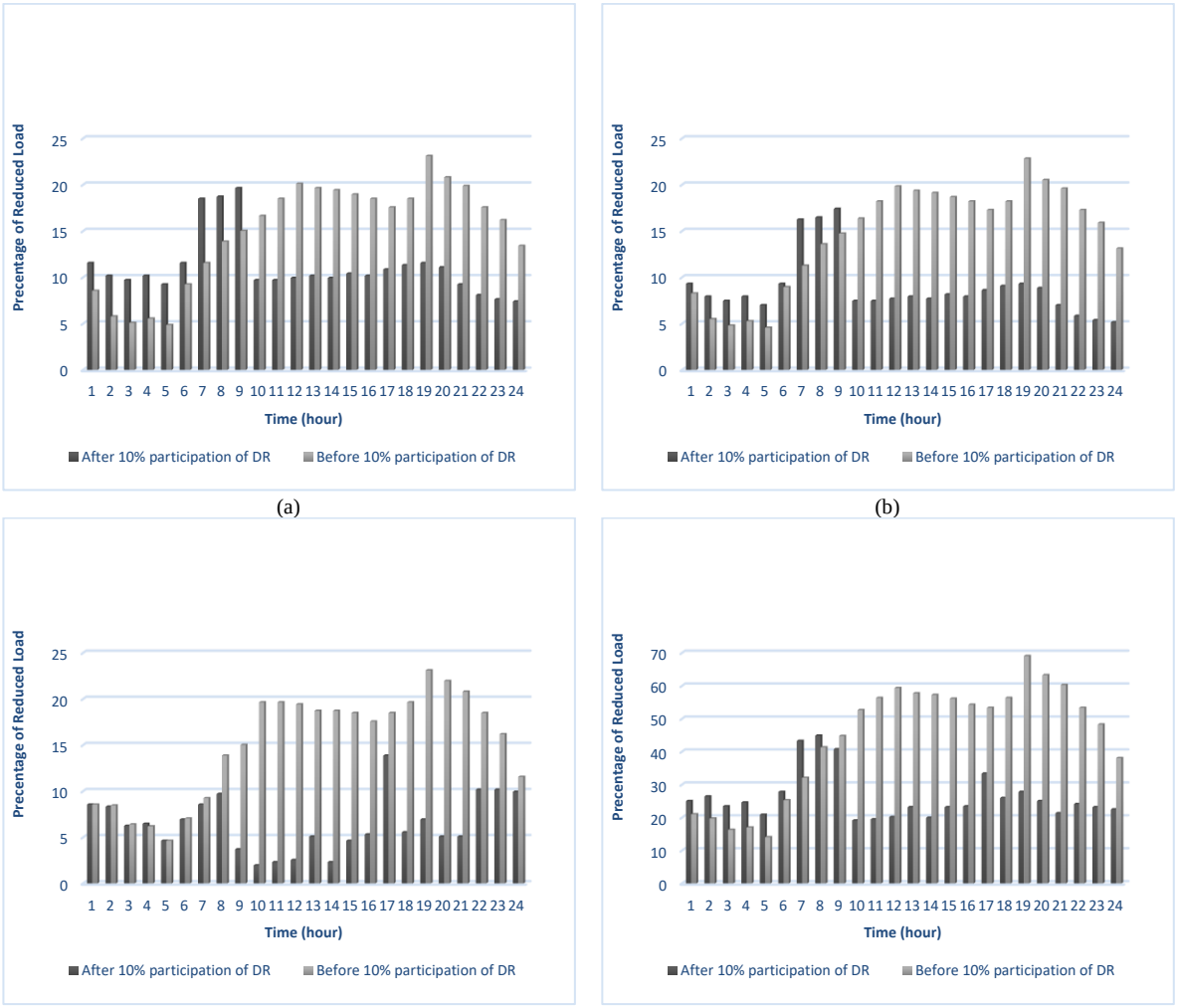

Fig. 10. Updated load for 10% participation of DR; a) TOU, b) RTP, c) CCP and d) total load

Case 1: Using Interruptible Load for 5% Participation in TOU Program

In contrast to the preceding section where the cost incurred by loads for electrical energy supply remained constant at 45,793.5 cents, the current section introduces a paradigm shift. Here, loads willingly engage in participation within TOU) programs, ushering in a dynamic where costs and benefits are subject to fluctuation based on participation decisions. The primary focus of this section is the comparative analysis of costs borne by loads before and after their voluntary participation in TOU programs, as elaborated in Table (2). These TOU programs operate on a voluntary basis and necessitate meticulous design to ensure that the benefits accruing from load participation exceed the total costs allocated to the resources.

This condition is essential for not only incentivizing future participation but also augmenting the revenue streams for loads engaging in these programs. This design approach, where the economic incentive for load participation is optimized, serves as a crucial motivator for loads to actively engage in TOU programs. Such initiatives not only create financial gains for participating loads but also contribute to the overall efficiency and economic viability of the energy distribution system

Case 2: Using Interruptible Load for 10% Participation in TOU Program

In the previous section, we shift our focus to the cost dynamics of responsive demands, emphasizing their participation in DRP. Specifically, we assess the financial implications for responsive demands both before and after their integration into the program, as elaborated in Table (3). It is crucial to note that this assessment illuminates the economic rationale behind the DRP's design. Upon meticulous examination, it becomes evident that the cost incurred after participation exceeds the cost incurred prior to participation across all three programs. This observation underscores the effectiveness of the DRP's design, which has successfully incentivized responsive

demands to engage. The determination of the interruptible load's value is a pivotal component of the optimization process, a parameter noted for its inherent variability. This value shall be provided in subsequent sections to offer a more comprehensive understanding of the system's intricacies. Furthermore, the total cost function value within this operational mode is quantified at 12,679.66 cents. This metric encapsulates the overall economic landscape influenced by responsive demand participation in DRP.

C) Scenario 3; Uncertainty Effect on DRPs Using IGDT

In this section, the uncertainty surrounding the participation of responsive demands in the programs is addressed through a modeling approach presented in Section 2, leveraging the info-gap theory. In prior sections, scenarios involving interruptible load ranged from 0% to 10%, while scenarios for responsive demands spanned participation rates between 5% and 10%. These scenarios were utilized to illustrate the effects of altering participation rates on the outcomes of the objective function. To comprehensively assess the influence of participation rate variability on the objective function results, a total of three distinct scenarios were modeled for responsive demands, as outlined in Table (4). These scenarios were designed to encapsulate a range of participation rates, thereby highlighting the dynamic nature of responsive demand behavior within the studied context. The results of the objective function for these four distinct scenarios have been meticulously compiled and are presented in Table 5. This tabulated data provides valuable insights into the implications of varying participation rates on the overall system's performance and cost-effectiveness.

As observed in the preceding table, altering the participation rate scenario exerts a relatively minor influence on the objective function value in the initial step but significantly impacts it in subsequent stages. This underscores the imperative of accounting for participation rate uncertainty, given the unconventional behavior exhibited by the objective function in response to varying load participation rates in the programs. Given that uncertainty in load participation rates typically exerts a negative impact on the objective function, a risk-averse decision-making strategy rooted in the principles of the info-gap theory is warranted. The objective here is to fortify the objective function's resilience against deviations in the participation of responsive demands from their predicted values. Thus, we proceed to solve the problem while employing a risk-aversion strategy, assuming a 10% deviation in the participation of responsive demands from their planned values (10%). Upon inspection of Table 7, it becomes apparent that a 10% deviation in responsive demand participation translates to an approximately 40% deviation from the base objective function value (i.e., objective function 12,060 for 10% participation of each load). Such a substantial deviation necessitates mitigation measures. In this section, we undertake a sensitivity analysis, encompassing key parameters, including the radius of uncertainty concerning the participation of responsive demands in the program (γ), the permissible radius of deviation of the objective function from the base value (θ), and various values of the LOLP. Notably, the value of the radius of uncertainty is evenly distributed between incentive-based and time-based loads. In the initial phase of sensitivity analysis, we consider variations in the permissible β value, ranging from 5% to 15% in increments of 2.5%, and alterations in the permissible LOLP value, ranging from 1% to 5% in increments of 1%. The determination of the radius of possible uncertainty required to meet the specified conditions is derived based on the insights gained from Figure 10.

Table.2.
The comparison of the cost of the loads participating in TOU programs before and after the implementation of the program (5%)

Program	*Average cost before DR participation (cents)*	*Average cost after DR participation (cents)*
TOU	1686.864	1520.229
RTP	1258.030	1022.785
CPP	1118.823	768.739

Table.3.
The comparison of the cost of the loads participating in TOU programs before and after the implementation of the program (10%)

Program	*Average cost before participation (cents)*	*Average cost after participation (cents)*
TOU	3373.728	3040.457
RTP	2516.061	2045.571
CPP	2237.647	1537.479

Table.4.
Total cost of objective function for different demand response scenarios

Objective function (censt)	*TOU program*	*Incentive-based program*
16902	0	0
16423	5 %	10 %
12060	10 %	10 %

Continuing with the sensitivity analysis on the problem parameters, this study explores the equitable distribution of the radius of uncertainty between incentive-based and time-based loads.

The findings, as illustrated in the figure, reveal a discernible trend: as the desired LOLP value decreases, the associated uncertainty radius pertaining to load participation also diminishes. In essence, a reduced level of uncertainty can be accommodated when aiming to uphold a stricter permissible LOLP threshold. Conversely, when the permissible percentage of increase in the objective function (θ) is elevated, a larger uncertainty radius can be tolerated while maintaining a predefined LOLP value. Building upon these insights, we proceed to investigate the impact of variations in the permissible uncertainty radius for changes in β, following the incremental steps outlined in the previous section. This analysis is conducted across various LOLP values, yielding the results depicted in Figure 11. In the subsequent phase of our analysis, we extend our examination by plotting Figure 12. Here, the horizontal axis, originally representing the value of the objective function, is replaced by the percentage of its deviation. This alternative visualization provides a deeper perspective on the relationship between the permissible uncertainty radius, LOLP values, and the percentage deviation of the objective function. These analyses collectively contribute to a nuanced understanding of the interplay between load participation uncertainty, permissible LOLP thresholds, and the tolerance for objective function variation. Such insights are invaluable in the context of decision-making and risk management within the framework of demand response programs and power distribution systems. Figure (12) illustrates a notable trend: as the permissible LOLP limit decreases, the corresponding uncertainty radius exhibits a reduction. Furthermore, it is evident that the sensitivity of the permissible uncertainty radius to variations in the permissible increase of the objective function (θ) becomes negligible when θ assumes small values. This observation underscores the relationship between the stringency of LOLP constraints and the degree of uncertainty tolerated in load participation. Specifically, as more stringent LOLP limits are imposed, the system requires a more precise and predictable response from load participants, resulting in a reduced uncertainty radius. Conversely, at smaller values of θ, which represent a greater tolerance for objective function variations, the sensitivity of the uncertainty radius to changes in θ diminishes. It is worth mentioning that the maximum LOLP is considerd as 6.5% in this research.

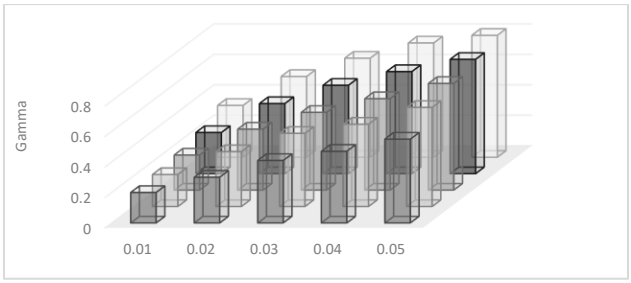

Fig. 11. Changes in the uncertainty in terms of LOLP changes for different θ

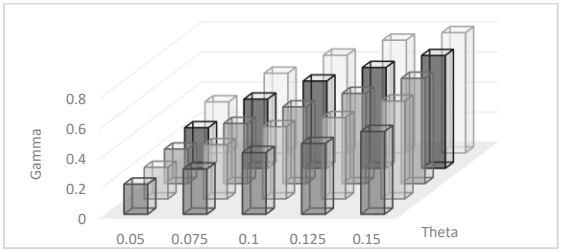

Fig. 12. Changes in the uncertainty in terms of θ changes for different LOLPs

These findings hold practical significance in the realm of decision-making and risk management within demand response programs and power distribution systems. They highlight the trade-offs between reliability (as reflected in LOLP constraints) and flexibility (as denoted by θ) and offer valuable insights for optimizing system performance while managing uncertainties. Increasing the desired LOLP for a given uncertainty radius results in higher operating costs imposed on the system. This signifies that achieving a lower desired LOLP alongside a larger uncertainty radius necessitates incurring a greater operational expense. In generan analyzing the changes in the uncertainty of microgrids, particularly concerning renewable energy resources, and their impact on Loss of Load Probability (LOLP) involves examining both the variations in θ and the LOLP for different scenarios. Let's break down the comparison into two aspects:
Changes in Uncertainty (Renewable Energy Resources) for Different θ:

- Low θ results in:
- High uncertainty in renewable energy resources may lead to increased LOLP at low costs.
- Limited financial resources might result in less robust backup systems or insufficient energy storage, amplifying the impact of renewable energy variability.
- Medium θ results in:
- A balance between costs and robustness is crucial. Moderate uncertainty may be manageable with appropriate investments in backup systems and storage.
- The LOLP may be influenced by the effectiveness of predictive models and control

systems in adapting to renewable energy fluctuations.
- High θ results in:
- Higher costs may provide resources for advanced technologies, such as improved energy storage or more sophisticated control systems.
- The LOLP could decrease as the system becomes more resilient to uncertainties, but there is a diminishing return on investment.

Changes in θ for Different LOLP Changes:
- Low LOLP results in:
- Low LOLP indicates a robust and reliable microgrid system.
- Initial investment might be high to ensure the reliability of the system, but operational costs may be lower due to fewer instances of load shedding.

Medium LOLP results in:
- A balance between costs and reliability is maintained.
- Investments in renewable energy forecasting, demand response, and energy storage could contribute to managing moderate LOLP without excessive costs.

High LOLP results in:
- High LOLP suggests potential issues with reliability and an increased need for investments.
- Additional costs θ may be required to improve backup systems, implement redundancy, or enhance energy storage capacity.

To assess the advantage of employing a risk-aversion strategy, we compare the following two operational modes:

The first mode: As previously mentioned, the system's cost is initially estimated at 12,060 units, assuming the participation of responsive demands according to predictions. However, we now assume that the actual load contribution deviates from predictions and aligns with the risk-aversion strategy's specifications (a 5% deviation for each responsive demand). Factoring in this modification while considering the existing spinning reserve, the total system cost amounts to 13,982 units. This represents an increase of 1,922 units compared to the baseline mode.

The second mode: In contrast to the first mode, we assume that the predicted 10% participation of responsive demands aligns with the planning obtained from the risk-aversion strategy, which incorporates a 5% deviation radius for each load. In this scenario, the cost of supplying the system load totals 12,611 units, indicating a cost reduction of 410 units compared to the risk-aversion strategy's cost.

The cost reduction observed in the second mode is less than the cost increase witnessed in the first mode. This indicates that employing a risk-aversion strategy exposes the grid operator to the risk of a relatively lower cost increase compared to the baseline mode. Furthermore, in the first mode, when the predicted output power values are not realized, the actual cost of 13,982 units exceeds the cost of 13,021 units obtained from the risk-aversion strategy. This observation suggests that the system operator may incur higher costs in real operating conditions than those anticipated through the risk-aversion strategy, particularly if uncertainties related to load participation are not adequately considered in the DRPs. These findings emphasize the economic implications of load participation uncertainties and underscore the potential benefits of incorporating risk-aversion strategies in power grid operation and management. They highlight the value of proactive planning and risk mitigation in optimizing system performance while managing uncertainties effectively.

D) Scenario 4; CVR Effect Objective Function

In this section, we provide a comprehensive overview of the grid under investigation, including its topology and technical specifications pertaining to its transmission lines. Specifically, the grid adheres to the IEEE standard 13-band configuration, which serves as the basis for its design and operation. Additionally, the hourly load profile, as previously outlined in the preceding sections, is incorporated into our study. Notably, this study encompasses a holistic examination of the grid, extending beyond the load profile analysis. Consequently, we employ the ZIP (ZIP load, Interruptible, and Price Elastic) model to represent the load distribution within the grid. It is essential to underscore that the final load consumed is subject to slight reductions in comparison to the initial load. This reduction stems from the load's dependency on the voltage levels within the system. To facilitate a detailed assessment of the load characteristics and their variation, we calculate the hourly load profiles, contrasting the conditions before the implementation of CVR and after the application of DR measures. These calculations are in accordance with Figure (13), which presents the load profile dynamics subsequent to the integration of CVR within the grid. It seems that actual load after CVR implementation is 11% decreased in average.

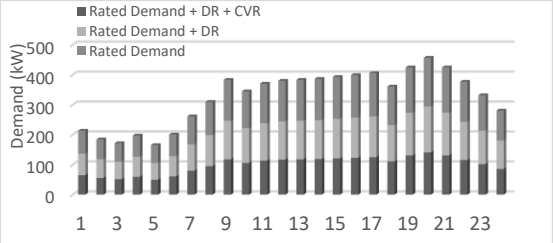

Fig. 13. Comparison of hourly load before and after applying CVR and DR

Below is an illustrative table comparing the cost minimization effects of pure CVR and pure DR along with a combined implementation of both CVR and DR:

- Pure CVR (Conservation Voltage Reduction): This implementation resulted in a cost minimization of 11.75%. CVR is known for its effectiveness in optimizing power distribution systems by adjusting voltage levels, thus improving overall energy efficiency.
- Pure DR (Demand Response): The pure DR implementation achieved a cost minimization of 16.98%. DR involves modifying electricity consumption patterns based on demand signals, contributing to cost reduction during peak demand periods.
- CVR + DR Combined: Implementing both CVR and DR simultaneously led to the highest cost minimization, with a reduction of 22.34%. This combined approach leverages the strengths of both strategies, potentially mitigating the challenges associated with the consumer-dependent nature of DR.

While pure DR is acknowledged for its potential, its effectiveness may vary based on consumer behavior and other external factors. Combining CVR and DR offers a more comprehensive and robust solution, balancing the advantages of each strategy and providing a more stable and adaptable approach to cost minimization in power systems. This comparison suggests that a combination of CVR and DR could be a strategic and effective approach to achieve a higher level of cost minimization in the power system, addressing the limitations associated with pure DR implementation.

Table.5.
Comparison for the effect of pure CVR and pure DR implementation for cost minimization

Implementation	***Cost Minimization (%)***
Pure CVR	11.75
Pure DR	16.98
CVR + DR Combined	22.34

4. Conclusion

The incorporation of CVR into the planning of microgrids represents a pivotal stride in the pursuit of sustainable and energy-efficient power distribution systems. By optimizing voltage levels while upholding power quality standards, microgrids featuring CVR pave the way for a reduction in energy consumption, an augmentation in grid reliability, and the facilitation of renewable energy source integration. Addressing the challenges linked to the implementation of CVR is imperative for realizing the complete potential of microgrids within the contemporary energy landscape. To facilitate further research in this domain, the following proposal is put forth:

- It is recommended that the correlation between uncertain sources, such as load, wind, and radiation scenarios, should be factored into the production of these scenarios. Moreover, it is advisable not to dismiss the practical uncertainties in the interplay between these factors when solving the problem.
- It is proposed that the pricing of load response programs should be structured in alignment with the disparity values between the worst-case scenario and the average scenario. This approach enables more effective load reduction and shifting during periods when such actions are required.
- Given the robustness of the IGDT method in addressing uncertainties, it is recommended that uncertainties associated with wind, load, and stress be modeled using this method rather than relying on scenario-based modeling. Subsequently, the results should be rigorously evaluated for their effectiveness and accuracy.

Nomenclature

Indices	
i	Number of generators
t	Time slots
n_{WT}	Number of wind turbines
Functions	
f_i^{WT}	The function of converting wind speed to wind turbine generation
f_i^{PV}	The function of converting the radiation value into photovoltaic generation
Variables	
$P_{i,t}$	The generation rate of unit i at time t
$Cost_{gen}$	Generation cost
$Cost_{res}$	Spining reserve cost

$Cost_{rel}$	Reliability cost
$U_{i,t}$	Binary variable of starting unit i at time t
$K_{i,t}$	Binary variable of unit i being turned on at time t
$\Delta P_{s,t}$	Change in available power due to event s at time t
$\Delta R_{s,t}$	Change of available reservation due to event s at time t
R_t	Total reservation at time t
$p_{s,t}$	The probability of event s at time t
$b_{s,t}$	Binary variable of load shedding due to event s at time t
$C(t)$	The energy in the battery at time t
$EENS$	The expected amount of energy not supplied
$LOLP$	The possibility of load shedding
$R_{i,t}$	The amount of reservation of unit i at time t
P_t^E	Battery generation or consumption power
Parameters	
$C_{i,t}$	Baseline generation cost per MW
$q_{i,t}$	Spining reservation cost per MW
SC_i	The cost of setting up unit i
$VOLL$	Lost load value
$LOLP_t^{max}$	The maximum probability of acceptable load shedding at time t
P_t^D	Load value at time t
P_i^{max}	Generation capacity of unit i
P_i^{min}	The minimum generation by unit i
RUR_i	The maximum slope of the increase in the generation by unit i
τ	Time steps
$v_{i,t}^{actual}$	The actual wind speed value at time t
$v_{i,t}^{fcst}$	The forecasted wind speed value at time t
$g_{i,t}^{fcst}$	The forecasted radiation value at time t
$g_{i,t}^{trun}$	The true radiation value at time t
P_{max}^E	The maximum battery capacity
d_T	Battery charge efficiency
C_S	Initial battery charge
C_E	Final battery charge
C_{min}	The minimum battery capacity
C_{max}	The maximum battery capacity
du_T	Duration of each failure

References

[1] Xu, J., Xie, B., Liao, S., Ke, D., Sun, Y., Jiang, X., & Yu, J. (2022). CVR-based real-time power fluctuation smoothing control for distribution systems with high penetration of PV and experimental demonstration. IEEE Transactions on Smart Grid, 13(5), 3619-3635.

[2] Zhang, Q., Guo, Y., Wang, Z., & Bu, F. (2021). Distributed optimal conservation voltage reduction in integrated primary-secondary distribution systems. IEEE Transactions on Smart Grid, 12(5), 3889-3900.

[3] Constante, G., Abillama, J., Illindala, M., & Wang, J. (2019). Conservation voltage reduction of networked microgrids. IET Generation, Transmission & Distribution, 13(11), 2190-2198.

[4] Nourollahi, R., Salyani, P., Zare, K., Mohammadi-Ivatloo, B., & Abdul-Malek, Z. (2022). Peak-load management of distribution network using conservation voltage reduction and dynamic thermal rating. Sustainability, 14(18), 11569.

[5] Gorjian, A., Eskandari, M., & Moradi, M. H. (2023). Conservation Voltage Reduction in Modern Power Systems: Applications, Implementation, Quantification, and AI-Assisted Techniques. Energies, 16(5), 2502.

[6] Singh, S., Barnwal, A. K., & Verma, M. K. (2022). Optimal charging of electric vehicles for cost minimization in re-configurable active distribution network considering conservation voltage reduction. Energy Sources, Part A: Recovery, Utilization, and Environmental Effects, 44(4), 10135-10155.

[7] Choeum, D., & Choi, D. H. (2020). Vulnerability assessment of conservation voltage reduction to load redistribution attack in unbalanced active distribution networks. IEEE Transactions on Industrial Informatics, 17(1), 473-483.

[8] Fakour, A., Jodeiri-Seyedian, S. S., Jalali, M., Zare, K., Tohidi, S., Zadeh, S. G., & Shafie-Khah, M. (2023). Investigating impacts of CVR and demand response operations on a bi-level market-clearing with a dynamic nodal pricing. IEEE Access, 11, 19148-19161.

[9] Thirunavukkarasu, G. S., Seyedmahmoudian, M., Jamei, E., Horan, B., Mekhilef, S., & Stojcevski, A. (2022). Role of optimization techniques in microgrid energy management systems—A review. Energy Strategy Reviews, 43, 100899.

[10] Azeem, O., Ali, M., Abbas, G., Uzair, M., Qahmash, A., Algarni, A., & Hussain, M. R. (2021). A comprehensive review on integration challenges, optimization techniques and control strategies of hybrid AC/DC Microgrid. Applied Sciences, 11(14), 6242.

[11] Constante, G., Abillama, J., Illindala, M., & Wang, J. (2019). Conservation voltage reduction of networked microgrids. IET Generation, Transmission & Distribution, 13(11), 2190-2198.

[12] Khalili, T., Jafari, A., Kalajahi, S. M. S., Mohammadi-Ivatloo, B., & Bidram, A. (2020, October). Simultaneous demand response program and conservation voltage reduction for optimal operation of distribution systems. In 2020 IEEE Industry Applications Society Annual Meeting (pp. 1-8).

[13] El-Shahat, A., Haddad, R. J., Alba-Flores, R., Rios, F., & Helton, Z. (2020). Conservation voltage reduction case study. IEEE Access, 8, 55383-55397.

[14] Mortazi, A., Saeed, S., & Akbari, H. (2023). Optimizing Operation Scheduling in a Microgrid Considering Probabilistic Uncertainty and Demand Response Using Social Spider Algorithm. International Journal of Smart Electrical Engineering, 12(02), 113-125.

[15] Mohammadjafari, M., Ebrahimi, R., & Parvin Darabad, V. (2019). Optimal economic operation and battery sizing for microgrid energy management systems considering demand response. International Journal of Smart Electrical Engineering, 8(04), 129-136.

[16] Apornak, K., Soleymani, S., Faghihi, F., & Mozafari, B. (2020). Optimal Modelling for Decision Making of Electricity Retailer in Power Market Contracts by Considering Demand Side Management Programs. International Journal of Smart Electrical Engineering, 9(01), 23-32.
[17] Kanakadhurga, D., & Prabaharan, N. (2022). Demand side management in microgrid: A critical review of key issues and recent trends. Renewable and Sustainable Energy Reviews, 156, 111915.
[18] Singh, A. R., Ding, L., Raju, D. K., Kumar, R. S., & Raghav, L. P. (2021). Demand response of grid-connected microgrid based on metaheuristic optimization algorithm. Energy Sources, Part A: Recovery, Utilization, and Environmental Effects, 1-22.
[19] Vijayan, V., Mohapatra, A., & Singh, S. N. (2020, December). A metaheuristic approach for conservation voltage reduction in unbalanced active distribution networks. In 2020 21st National Power Systems Conference (NPSC) (pp. 1-6). IEEE.
[20] Zhou, B., Zou, J., Chung, C. Y., Wang, H., Liu, N., Voropai, N., & Xu, D. (2021). Multi-microgrid energy management systems: Architecture, communication, and scheduling strategies. Journal of Modern Power Systems and Clean Energy, 9(3), 463-476.
[21] Wang, Z., & Wang, J. (2013). Review on implementation and assessment of conservation voltage reduction. IEEE Transactions on Power Systems, 29(3), 1306-1315.
[22] Zhang, Y., Ren, S., Dong, Z. Y., Xu, Y., Meng, K., & Zheng, Y. (2017). Optimal placement of battery energy storage in distribution networks considering conservation voltage reduction and stochastic load composition. IET Generation, Transmission & Distribution, 11(15), 3862-3870.
[23] Sandraz, J. P. A., Macwan, R., Diaz-Aguiló, M., McClelland, J., De León, F., Czarkowski, D., & Comack, C. (2014). Energy and economic impacts of the application of CVR in heavily meshed secondary distribution networks. IEEE transactions on power delivery, 29(4), 1692-1700.
[24] Varshney, H., Jain, H., & Tiwari, R. (2023). Thermal-Electric Modeling: A New Approach for Evaluating the Impact of Conservation Voltage Reduction on Cooling Equipment. Buildings, 13(5), 1287.
[25] Mehdizadeh, A., Taghizadegan, N., & Salehi, J. (2018). Risk-based energy management of renewable-based microgrid using information gap decision theory in the presence of peak load management. Applied energy, 211, 617-630.
[26] Hossan, M. S., & Chowdhury, B. (2019). Integrated CVR and demand response framework for advanced distribution management systems. IEEE Transactions on Sustainable Energy, 11(1), 534-544.